

Structural And Morphological Analysis of $Y(\text{Ta,Nb})\text{O}_4:\text{Eu}^{3+},\text{Tb}^{3+}$ Phosphors

I. D. Arellano^{1*}, M. Nazarov^{1,2}, Do Young Noh¹

¹ Department of Materials Science and Engineering, Gwangju Institute of Science and Technology, 1 Oryong-dong, Buk-gu, Gwangju 500-712, Republic of Korea

² Institute of Electronic Engineering and Industrial Technologies, Academy Sciences of Moldova, Republic of Moldova

Recibido 22 de Oct. 2007; Aceptado 15 de Oct. 2008; Publicado en línea 5 de Ene. 2009

Resumen

Itrio tantalio (YTaO_4), itrio niobio-tantalio (YTaNbO_4) y itrio niobio (YNbO_4), son eficientes fósforos de rayos X. La influencia de los iones de tierra rara tales como Eu^{3+} y Tb^{3+} en la estructura cristalina y la morfología de estos fósforos fueron estudiadas. Las estructuras $\text{Y}(\text{Ta,Nb})\text{O}_4$ simultáneamente activadas por Eu^{3+} and Tb^{3+} fueron investigadas por medio de difracción de rayos X (DRX) y de espectroscopia infraroja con transformada de Fourier (FT-IR) con el fin de ampliar el conocimiento de las propiedades estructurales de estos materiales doblemente activados. La morfología de los fósforos preparados fue caracterizada por el microscopio electrónico de barrido (SEM). El método de Rietveld se llevo a cabo con el fin de calcular los datos cristalográficos de los fósforos investigados.

Palabras claves: YTaO_4 , YNbO_4 , fósforos, DRX, FT-IR, método de Rietveld.

Abstract

Yttrium tantalate (YTaO_4), yttrium niobium-tantalate (YTaNbO_4) and yttrium niobate (YNbO_4), are efficient X-ray phosphors. The influence of the rare earth ions such as Eu^{3+} and Tb^{3+} on the crystalline structure and morphology of these phosphors were studied. The doubly activated simultaneously $\text{Y}(\text{Ta,Nb})\text{O}_4$ structures by Eu^{3+} and Tb^{3+} were investigated by means of X-ray diffraction and Fourier transform infrared spectroscopy (FT-IR) in order to enlarge the knowledge of the structural properties of these doubly activated materials. Morphology of the prepared phosphors was characterized by scanning electron microscope (SEM). Rietveld refinement was done in order to calculate the crystallographic data of investigated X-ray phosphors.

Keywords: YTaO_4 , YNbO_4 , phosphors, XRD, FT-IR, Rietveld refinement.

© 2009 Revista Colombiana de Física. Todos los derechos reservados.

1. Introduction

Yttrium tantalate has three crystal structures; high temperature ($>1450^\circ\text{C}$) tetragonal (scheelite, T-structure), low temperature (about 1000°C) monoclinic (fergusonite, M-structure) and another monoclinic form called M' that can be synthesized at lower temperatures (below 1400°C) [1,2]. M' transforms to T at approximately 1450°C and then to M upon cooling. It is M' modification that is used in phosphor screens. The M' yttrium tantalate structure is an efficient

host lattice for X-ray phosphors when activated with niobium or rare earth (RE), in comparison with the monoclinic yttrium tantalate (M- YTaO_4). The unit cell parameters for M'- YTaO_4 are $a = 5.29 \text{ \AA}$, $b = 5.45 \text{ \AA}$, $c = 5.11 \text{ \AA}$, and $\beta = 96.45^\circ$, and the density is 7.57 g/cm^3 [3,4].

In M'- YTaO_4 structure, tantalum atoms are in a distorted octahedral coordination with six Ta-O bonds whereas in M- YTaO_4 tantalum atoms are in tetrahedral coordination [3,5]. These distorted TaO_6 units share edges with one another to form strings. Yttrium atoms are surrounded by 8-

coordinated oxygen atoms forming a distorted cube. The total number of atoms inside of the $M'-YTaO_4$ structure is: 2 yttrium atoms, 2 tantalum and 8 oxygen atoms [6]. The niobium atoms of the fergusonite $M'-YNbO_4$ structure present the same octahedral coordination with six Nb-O bonds such $M'-YTaO_4$.

Different rare earth activators such as Eu^{3+} , Tb^{3+} , Gd^{3+} , Sm^{3+} , Dy^{3+} , Pr^{3+} were used in previous works to replace the yttrium ions into the $YTaO_4$ or $YNbO_4$ crystalline structure [7,8]. However, the morpho-structural properties of $Y(Ta,Nb)O_4$ doubly activated by rare earth elements have not been studied yet. In the present study, the rare earth activators such as Eu^{3+} and Tb^{3+} were simultaneously incorporated into $M'-YTaO_4$, $M'-YTaNbO_4$ and $M'-YNbO_4$ structures. These powder samples were investigated by means of XRD and FT-IR in order to study their structural properties. The crystallographic data for these phosphors were calculated using refinement method.

2. Experimental part

$Y(Ta,Nb)O_4$ doubly activated by Eu^{3+} and Tb^{3+} were prepared by solid state reaction method from homogeneous mixture consisting of Y_2O_3 , Ta_2O_5 and Nb_2O_5 . Eu_2O_3 and/or Tb_4O_7 were used in the activator system and Na_2SO_4 as

flux. The crystal structure of the prepared materials were determined by an X-ray diffractometer (Rigaku), we measured the powder diffraction profiles (θ - 2θ scan) covering the range between 10° and 80° . The morphological analysis was performed by scanning electron microscope (SEM) Hitachi S-4700. The infrared absorption spectra at room temperature were measured using a Perkin Elmer FT-IR spectrometer spectrum 2000 in the spectral range 400 - 1000 cm^{-1} , the KBr pellets techniques were used.

Two types of host lattices (M' and M) with double activation by rare earth elements Eu^{3+} and Tb^{3+} were prepared. General formula of the phosphors is $Y_{1-x-y}Eu_xTb_yTa_{1-z}Nb_zO_4$, denoted as $Y(Ta,Nb)O_4:Eu^{3+},Tb^{3+}$. For the samples we measured, $x=0.025$, $y=0.025$ and $z=0$; 0.15 or 1 . The chemical compositions of prepared phosphor samples are listed in Table 1.

3. Results and discussion

3.1 Particle morphology

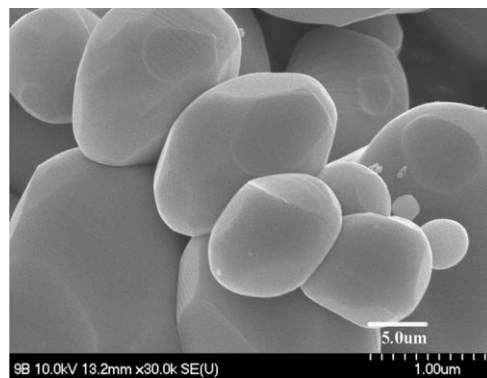
Using a scanning electron microscope, we observed stone-like morphologies of $YTaO_4:Eu^{3+},Tb^{3+}$ and $YNbO_4:Eu^{3+},Tb^{3+}$ (Fig. 1).

Table No.1 Composition of yttrium tantalate/niobate phosphors with double activation by Eu^{3+} and Tb^{3+}

Phosphor type	Phosphor formula	Host lattice (mol%)		RE-activator (mol%)	
		$YTaO_4$	$YNbO_4$	Eu^{3+}	Tb^{3+}
$M'-YTaO_4:Eu,Tb$	$Y_{0.95}Eu_{0.025}Tb_{0.025}TaO_4$	100	-	2.5	2.5
$M'-YTaNbO_4:Eu,Tb$	$Y_{0.95}Eu_{0.025}Tb_{0.025}Ta_{0.85}Nb_{0.15}O_4$	85	15	2.5	2.5
$M'-YNbO_4:Eu,Tb$	$Y_{0.95}Eu_{0.025}Tb_{0.025}NbO_4$	-	100	2.5	2.5



(a)



(b)

Fig.1 SEM images of phosphor samples a) $YTaO_4:Eu^{3+},Tb^{3+}$ b) $YNbO_4:Eu^{3+},Tb^{3+}$

From Fig. 1, it can be seen that the samples mainly consist of solid, uniform and non-agglomerated crystalline particles. For $\text{YTaO}_4:\text{Eu}^{3+},\text{Tb}^{3+}$ the crystalline grain has elongated polyhedral form, the particles are estimated to be around 3 to 5 μm . The grain size increases for $\text{YNbO}_4:\text{Eu}^{3+},\text{Tb}^{3+}$ to be around 10 μm in dimension, having a polyhedral more round shape. Such micrometer dimensions for these powders are rather desirable particles size range, since larger particles begin to cause difficulty in making X-ray screen, and much smaller particles will lose emission intensity via internal scattering as the particle size gets much below 3 μm .

The scanning electron microscope shows the physical difference between $\text{M}'\text{-YTaO}_4$ and $\text{M}'\text{-YNbO}_4$ structures.

3.2 XRD crystalline structure characterization

The X-ray diffraction (XRD) spectra of three different phosphors doubly activated by Eu^{3+} and Tb^{3+} are shown in Figure 2. The $\text{M}'\text{-YTaO}_4$ XRD pattern is shown in Fig. 2(a). X-ray diffraction spectrum of $\text{YNbO}_4:\text{Eu}^{3+},\text{Tb}^{3+}$ (Fig. 2(c)) shows the evidence of the monoclinic $\text{M}'\text{-YNbO}_4$ fergusonite crystal structure. Incorporation of 15% niobium atoms into the $\text{M}'\text{-YTaO}_4$ host lattice did not change the basic M' structure (Fig. 2(b)). The JCPDS card for $\text{M}'\text{-YTaO}_4$ completely coincides with the YTaNbO_4 measurement data. The black points (2) in Fig. 2 (a,b,c) are the measured data received from the XRD and the solid lines (1) are the calculated fitting of Rietveld analysis which was developed by Rietveld for structure profile refinement of X-ray powder diffraction data. The measured peak positions are in good agreement with Rietveld fitting (1) and data given in Powder Diffraction File JCPDS 72-2018 (For YTaO_4) and JCPDS 72-2077 (For YNbO_4) from International Center for Diffraction, (3).

The Rietveld calculation provides the crystallographic information by comparing the model profile with X-ray or

neutron curves using the least squares method. One uses Rietveld analysis generally to get the lattice parameters, atomic positions and atomic distances. The peak positions of X-ray diffraction curve are related to the unit cell lattice constants of the crystal structure and the peak intensities are affected by various parameters such as atomic position, atomic occupancy, and thermal effect. The detailed crystallographic information of the measured phosphors from Rietveld analysis is listed in Table 2 and Table 3. From the occupation factor F (Table 2), one can see that $F = 1$, which means the site is fully occupied by an atom.

3D pictures for the structures $\text{M}'\text{-YTaO}_4$ and $\text{M}'\text{-YNbO}_4$ doubly activated by Eu^{3+} and Tb^{3+} were created using the data from Table 2 and Table 3. These pictures are presented in Figure 3.

Fig. 3a illustrates the position of the rare earth activators Eu^{3+} and Tb^{3+} substituting yttrium atoms in the $\text{M}'\text{-YTaO}_4$ host lattice. In $\text{M}'\text{-YTaO}_4:\text{Eu}^{3+},\text{Tb}^{3+}$ the Y atoms (Fig. 3a) are surrounded by 8-coordinated oxygen atoms forming a distorted cube. The average Y-O distance from our calculations is 2.37 \AA . The tantalum atoms (Fig. 3a) are in a distorted octahedral coordination with four shorter Ta-O bonds at 1.96 \AA and 1.87 \AA and two longer at 2.23 \AA . In the same way, Fig. 3b shows the crystallographic structure of $\text{M}'\text{-YNbO}_4:\text{Eu}^{3+},\text{Tb}^{3+}$. The Y atoms are also surrounded by 8-coordinated oxygen atoms forming a distorted cube. The average Y-O distance is 2.35 \AA . The Nb atoms are in a distorted octahedral coordination with four shorter Nb-O bonds at 1.94 \AA and 1.83 \AA and two longer at 2.43 \AA .

The incorporation of the rare earth ions Eu^{3+} and Tb^{3+} into $\text{M}'\text{-YTaO}_4$ and $\text{M}'\text{-YNbO}_4$ did not change the basic crystal-line structures and the results do not differ so much from host lattices reported previously [3,6]. According to Vegard's law, the addition of the rare earth ions results to an increment in the unit cell volume from 146.57 to 147 \AA and 292.81 to 293.13 \AA for YTaO_4 and YNbO_4 , respectively

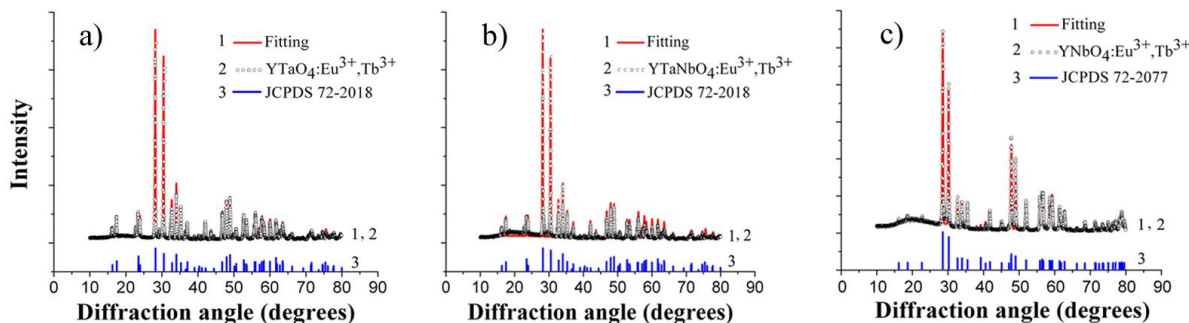


Fig.2 XRD patterns of: a) $\text{YTaO}_4:\text{Eu}^{3+},\text{Tb}^{3+}$; b) $\text{YTaNbO}_4:\text{Eu}^{3+},\text{Tb}^{3+}$; c) $\text{YNbO}_4:\text{Eu}^{3+},\text{Tb}^{3+}$. The results of fitting are shown by solid lines. Expected peak positions from JCPDS cards are indicated.

Table No.2 Atomic positions and lattice parameters for different host lattices

$M'-YTaO_4:Eu^{3+},Tb^{3+}$	Atom	x	y	z	F
a=5.298Å	Y	0.25	0.7605	0	1
b=5.461Å	Ta	0.25	0.3111	0.5	1
c=5.112Å	O(1)	0.4192	0.4033	0.3079	1
$\beta=96.37$	O(2)	0.1230	0.1117	0.2824	1
$M'-YTaNbO_4:Eu^{3+},Tb^{3+}$	Atom	x	y	z	F
a=5.299Å	Y	0.25	0.726	0	1
b=5.476Å	Ta	0.25	0.2611	0.5	1
c=5.072Å	O(1)	0.5251	0.4236	0.2746	1
$\beta=94.51$	O(2)	0.0857	0.0810	0.2140	1
$M'-YNbO_4:Eu^{3+},Tb^{3+}$	Atom	x	y	z	F
a=7.617Å	Y	0	0.3791	0.25	1
b=10.95Å	Nb	0	0.8551	0.25	1
c=5.298Å	O(1)	0.2286	0.79	0.2422	1
$\beta=138.42$	O(2)	0.2519	0.9576	0.6818	1

Table No.3 Interatomic distances between anions and cations of different host lattices

Structure	Y-O (Å)	Ta-O (Å)	Nb-O (Å)
$M'-YTaO_4:Eu^{3+},Tb^{3+}$	O(1) 2x 2.524	O(1) 2x 1.957	
	O(2) 2x 2.348	O(1) 2x 2.230	
	O(1) 2x 2.322	O(2) 2x 1.870	
	O(2) 2x 2.296		
$M'-YTaNbO_4:Eu^{3+},Tb^{3+}$	O(1) 2x 2.545	O(1) 2x 1.926	
	O(2) 2x 2.331	O(1) 2x 2.251	
	O(1) 2x 2.289	O(2) 2x 1.874	
	O(2) 2x 2.325		
$M'-YNbO_4:Eu^{3+},Tb^{3+}$	O(1) 2x 2.391		O(1) 2x 1.944
	O(2) 2x 2.331		O(1) 2x 2.426
	O(1) 2x 2.304		O(2) 2x 1.830
	O(2) 2x 2.387		

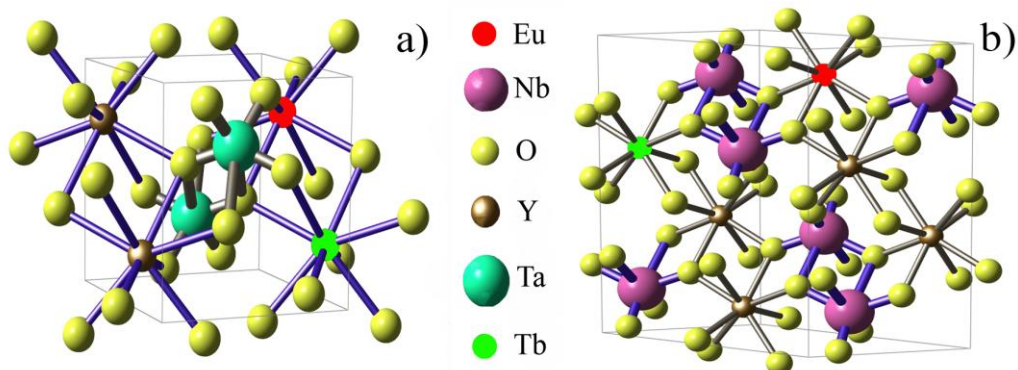


Fig.3 Crystal structures: a) $M'-YTaO_4$ and b) $M'-YNbO_4$. The substitution of Y ions by Eu^{3+} and Tb^{3+} is indicated.

3.3 FT-IR crystalline structure characterization

FT-IR spectroscopy was also used in order to prove the crystalline structure of investigated phosphors (Fig. 4).

We consider that the bands observed at 444 cm^{-1} and 650 cm^{-1} in Fig. 3a are assigned to degenerated $\nu(\text{Ta-O-Ta})$, and the band at 745 cm^{-1} to degenerated $\nu_{\text{asym}}(\text{Ta-O})$ vibration, that is in good agreement with data published by A. Hristea and others for YTaNbO_4 [9]. The infrared spectra of $\text{YTaNbO}_4:\text{Eu}^{3+},\text{Tb}^{3+}$ (Fig. 4b) support the idea that the crystalline host lattice of powder with niobium atoms concentration (15% mol) and rare earth activators (Eu^{3+} and Tb^{3+} , 5% mol) preserve the M' crystalline structure, as already was pointed out by X-ray diffraction. The infrared spectra suggest a good incorporation of niobium and Eu^{3+} and Tb^{3+} ions into the host crystalline lattice, i.e. a relatively homogeneous distribution of NbO_4^{3-} groups replaces TaO_4^{3-} groups into the M'- YTaNbO_4 crystalline matrix. In Fig. 4c, the totally replacement of TaO_4^{3-} groups by NbO_4^{3-} groups induces the conversion of M' into M phase, process that is shown by the shift of the 444 cm^{-1} and 650 cm^{-1} bands, and the disappearance of the 745 cm^{-1} band. Moreover, the infrared spectrum (Fig. 4c) contains different oscillation frequencies; ν_1 at 806 cm^{-1} and ν_3 at $670, 597$ and 543 cm^{-1} that are in agreement with M- YNbO_4 structure [10].

4. Conclusions

The detailed crystallographic data of the investigated M'- $\text{YTaNbO}_4:\text{Eu}^{3+},\text{Tb}^{3+}$, M'- $\text{YTaNbO}_4:\text{Eu}^{3+},\text{Tb}^{3+}$ and M- $\text{YNbO}_4:\text{Eu}^{3+},\text{Tb}^{3+}$ was estimated by means of Rietveld calculation. The X-ray diffraction patterns, sustained by infrared spectroscopy and scanning electron microscope put in evidence that the partially substitution of yttrium atoms by europium and terbium ions does not change essentially the morpho-structural characteristics of M'- YTaNbO_4 and M- YNbO_4 . The investigated powders doubly activated by Eu^{3+} and Tb^{3+} can be applied to the manufacture of X-ray intensifying screens used in medical diagnosis.

Acknowledgements

This work was supported by the Korean Science and Engineering Foundation (KOSEF) through National Research Laboratory (Program No. M10400000045-04J0000-04510).

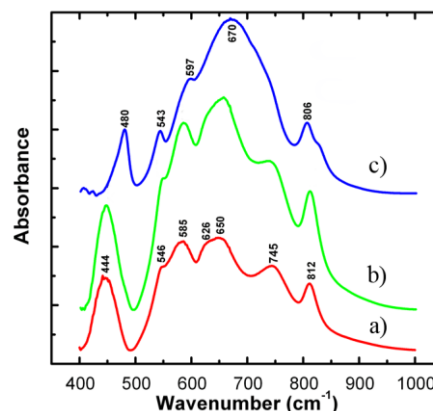


Fig.4 FT-IR spectra of: a) $\text{YTaNbO}_4:\text{Eu}^{3+},\text{Tb}^{3+}$; b) $\text{YTaNbO}_4:\text{Eu}^{3+},\text{Tb}^{3+}$; c) $\text{YNbO}_4:\text{Eu}^{3+},\text{Tb}^{3+}$.

References

- [1] L.H. Brixner, Mater. Chem. Phys. 16, 253-281, (1987).
- [2] G.M. Wolten, Acta Crystallogr. 23, 939-944, (1967).
- [3] L.H. Brixner and H. Chen, J. Electrochem. Soc. 130, 2435-2443, (1983).
- [4] V.K. Trunov, et al., Kristallografiya, 26, 67 (1981)
- [5] G. Blasse, L.H. Brixner, J. Solid State Chem. 82, 115-155, (1989)
- [6] S.L. Issler, C.C. Torardi, J. Alloy. Compd. 229, 54-65, (1995)
- [7] G. Blasse, A. Brill, J. Lumin. 3, 109-131, (1970)
- [8] W.J. Schipper, M.F. Hoogendorp, G. Blasse, J. Alloy. Compd. 202, 283-287, (1993)
- [9] Amalia Hristea, E.J. Popovici, Laura Muresan, Maria Stefan, Rodica Grecu, Anders Johansson, Mats Boman, J. Alloys and comp., 2008 (article in press)
- [10] K.I. Petrov, N.V. Gundobin, V.V. Kravchenko, S.S. Plotkin, J. Inorg. Chem. 18 (in russian), 928-930, (1973)